Mass Spectrometric Analysis of Posttranslational Modifications of a Carrot Extracellular Glycoprotein†

Chengwei Shang, Tadashi Shibahara, Kazuki Hanada, Yuko Iwafune, and Hisashi Hirano*

Kihara Institute for Biological Research, Graduate School of Integrated Science, Yokohama City University, Maioka-cho 641-12, Totsuka, Yokohama 244-0813, Japan

Received December 2, 2003; Revised Manuscript Received March 25, 2004

ABSTRACT: Expression of extracellular dermal glycoprotein (EDGP) is induced by biotic or abiotic stress. The amino acid sequence alignment showed that EDGP shared significant homology with proteins from legumes, tomato, *Arabidopsis*, wheat, and cotton. These proteins are involved in signal transduction or stress response systems. Most of the Cys residues in these proteins are conserved, suggesting that they share similar tertiary structures. Surface plasmon resonance (SPR) analysis shows that EDGP binds a soybean 4-kDa hormone-like peptide (4-kDa peptide) in vitro and reduction of EDGP decreased significantly the binding activity, implying that posttranslational modifications are important for its function. Therefore, we investigated the posttranslational modifications in EDGP using mass spectrometry. As the result, six disulfide bonds in EDGP were identified: Cys^{70}−Cys^{158}, Cys^{84}−Cys^{89}, Cys^{97}−Cys^{113}, Cys^{100}−Cys^{108}, Cys^{201}−Cys^{426}, and Cys^{332}−Cys^{378}. In addition, the N-terminal glutamine was cyclized into pyroglutamic acid. All four putative glycosylation sites were occupied by N-linked glycans, which have similar masses of *m*/*z* 1171. Finally, measuring the mass of the native protein showed that the posttranslational modifications of EDGP (p*I* 9.5) involved only disulfide bonds, N-terminal modification, and glycosylation.

Expression of the extracellular dermal glycoprotein (EDGP)[1] gene is induced by wounding the mature taproot (*1*), and expression of an Ageratum conyzoides gene (GenBank accession number BI397500), similar to the EDGP gene, is strongly upregulated when a plant is infected by *Agrobacterium tumefaciens* (*2*), suggesting that EDGP is involved in the response to biotic or abiotic stress. Amino acid sequence comparison shows that homologues of EDGP are widely present in plants, such as legume, wheat, and cotton. When soybean or lupine seeds are immersed in water at 50−60 °C, large amounts of the respective EDGP homologue proteins are released (*3*), suggesting that they are induced by stress. Another homologue protein has been purified from cottonseed and shows weak antifungal activity (*4*). A protein from wheat, a 25% homologue with EDGP, inhibits family 11 endoxylanases (*5*). Recently, it was reported that EDGP inhibits the activity of xyloglucan-specific β-1,4-endoglycanase (XEG) from fungus (*Aspergillus aculeatus*) by forming a mixture (*6*), suggesting that EDGP plays a protective role in plant cell walls.

Furthermore, a soybean 4-kDa hormone-like peptide (4-kDa peptide) competes with insulin to bind a 43-kDa protein (33% homologue with EDGP) in soybean and stimulates its protein kinase activity (*7*), suggesting that these compounds are involved in an insulin-like signal transduction pathway. EDGP binds also insulin in vitro (*8*) and localizes in the plasma membrane and middle lamellae of cell walls, which is similar to that of the 4-kDa peptide and the 43-kDa protein (*9*). This suggests that EDGPs have a role in the signal transduction system. However, it is not clear whether EDGP is the binding protein of the 4-kDa peptide.

From their primary amino acid sequences, EDGP homologues have two common properties: one is that most of their Cys residues are conserved and another is that they have putative N-linked glycosylation sites. These common points indicate that posttranslational modifications are important for their functions. However, the biochemical property of the homologues is unknown. In the present study, it was confirmed that EDGP was the 4-kDa peptide-binding protein in carrot, and reduction of EDGP caused the binding to significantly decrease, suggesting that posttranslational modifications of EDGP are important for maintaining its function. Therefore, to understand the biochemical property in detail, the posttranslational modifications of EDGP were analyzed using mass spectrometry.

EXPERIMENTAL PROCEDURES

Materials

The desalting column (PD-10 column) and low molecular marker kit were purchased from Amersham Biosciences (Piscataway, NJ). *N*-Ethylmaleimide (NEM), trypsin, chymotrypsin, and pepsin were obtained from Sigma-Aldrich Co. (St. Louis, MO). *Staphylococcus aureus* V8 protease and Tris-HCl (2-carboxyethyl)phosphine hydrochloride (TCEP) were purchased from Pierce (Rockford, IL). BIAcore X instrumentation, software, and reagents, including the NTA

† This research was supported by the Scholarship of the Ministry of Education, Culture, Sports, Science, and Technology, Japan.

* Corresponding author. Tel: +81-45-820-1904. Fax: +81-45-820-1901. E-mail: Hirano@yokohama-cu.ac.jp.

[1] Abbreviations: EDGP, extracellular dermal glycoprotein; NEM, *N*-ethylmaleimide; IAA, iodoacetic acid; SPR, surface plasmon resonance; 2,4-D, 2,4-dichlorophenoxyacetic acid; TCEP, Tris-HCl (2-carboxyethyl)phosphine hydrochloride.

10.1021/bi036160f CCC: $27.50
Published on Web 04/27/2004

sensor chip, were purchased from BIAcore (Uppsala, Sweden). Glycopeptidase A was from Seikagaku Co. (Tokyo, Japan). Iodoacetic acid (IAA) and the organic solutions used for HPLC were obtained from Wako Chemicals (Osaka, Japan). The His-tagged 4-kDa peptide was prepared according to Hanada et al. (*10*).

Methods

Culture of Carrot Callus. Suspension medium containing 1 mg/L 2,4-dichlorophenoxyacetic acid (2,4-D) was prepared for carrot cells (*11*). To the fresh medium was added mature carrot cell suspension (*Daucus carota* L.), and then the resultant suspension was cultured for 3 weeks at 25 °C.

Concentrating Proteins from Carrot Callus Suspension Culture Medium. The supernatant, collected from the 3-week-old carrot callus suspension culture medium by centrifugation, was filtered through filter paper, and solid ammonium sulfate was added up to 80% saturation. After incubation for a few hours at 4 °C, the precipitate was collected by centrifugation and dissolved in 20 mM sodium phosphate buffer containing 500 mM NaCl, pH 7.4. Then, a 0.45-μm filter (Millipore, Billeria, MA) was used to remove the insoluble aggregates. The concentration of the sample solution was measured using the Bradford assay (*12*), followed by surface plasmon resonance (SPR) analysis.

SPR Analysis. The BIAcore system and NTA sensor chip were used for the binding assay. The flow rate was 20 μL/min, and the running buffer was 20 mM sodium phosphate containing 0.5 M NaCl, pH 7.4. According to the supplier's instructions, $NiSO_4$ solution was passed through both the reference and target cells, and then 20 ng of the His-tagged 4-kDa peptide were immobilized in the target cell, while no peptide was immobilized in the reference cell. Sample solution, concentrated from carrot culture medium as described above, was passed through both cells. After both cells were washed and equilibrated with running buffer, 5 μL of 350 mM EDTA were used to elute the two cells. The data were obtained and analyzed using BIAevaluation software, version 3.2.

Identification of the 4-kDa Peptide-Binding Protein. The resultant fractions from the target cell in the NTA sensor chip were concentrated and subjected to SDS−PAGE. Then, they were transferred to poly(vinylidene difluoride) (PVDF) membrane using the method of Hirano and Watanabe (*13*) and subjected to western blotting with anti-EDGP antibody. The same eluent was also subjected to SDS−PAGE and then stained using a SilverQuest silver staining kit (Invitrogen, Carlsbad, CA). The visualized protein band was excised for in-gel digestion with trypsin followed by matrix-assisted laser desorption−time-of-flight mass spectrometry (MALDI-TOF MS; Micromass, Manchester, U.K.) as described previously (*14*).

Purification of EDGP. A published protocol for EDGP purification (*15*) was used with some changes. Briefly, 3-week-old carrot callus culture medium was centrifuged, and the supernatant was filtered through a 1-μm filter membrane. The resultant solution was adjusted to pH 4.6 and then applied to a strong cation-exchange column, which was equilibrated with 50 mM sodium acetate (NaOAc) buffer, pH 4.6. The proteins bound to this column were eluted with 500 mM NaCl in equilibration buffer, and then the sample buffer was exchanged for 50 mM NaOAc buffer (pH 4.6) using a PD-10 column. Then, the sample was applied to a prepacked strong cation-exchange column (Econo-Pac High S; Bio-Rad, Hercules, CA). The resultant fractions were checked by in-gel digestion followed by MALDI-TOF MS. The fractions containing EDGP were collected and dialyzed against 50 mM Tris-HCl buffer, pH 7.5, containing 1.0 M ammonium sulfate; then, the retentate was applied to a hydrophobic interaction column (Resource Phe; Amersham Biosciences), which was equilibrated with the equilibration buffer and eluted with a linear gradient of 1.0−0 M ammonium sulfate in 50 mM Tris-HCl buffer, pH 7.5. The fractions corresponding to the main peak were collected and subjected to a PD-10 column to change the buffer to 20 mM NaOAc, pH 4.6. Then, they were applied to another strong cation-exchange column (Uno S1; Bio-Rad), which was equilibrated with the binding buffer and eluted with a linear gradient of 0−300 mM NaCl in the binding buffer at pH 4.6. The eluent at the position of 200 mM NaCl was collected for this study.

Effect of EDGP Conformation on Binding with the 4-kDa Peptide. The purified EDGP (20 μL, 0.16 mg/mL) was passed through an NTA sensor chip, prepared as described above, at a flow rate of 10 μL/min. Then, the EDGP was completely reduced with 10 mM DTT at 37 °C for 30 min and labeled with 50 mM IAA at room temperature for 30 min. The reduced EDGP was desalted with a C4 column (4.6 × 100 mm; Nacalai Tesque Co., Kyoto, Japan) coupled with reverse-phase (RP) HPLC (Beckman, Palo Alto, CA). The fraction containing the denatured EDGP was collected, dried, resolved in the running buffer, and subjected to SPR analysis.

Ligand Blotting Assay. Ligand blotting analysis was used to analyze the interaction between the reduced EDGP and the 4-kDa peptide according to the method of Yamazaki et al. (*16*). The wild-type 4-kDa peptide was purified from soybean as described previously (*7*).

ESI-Q-TOF MS. Electrospray ionization−quadrupole−time-of-flight mass spectrometry (ESI-Q-TOF MS; Micromass) analysis was performed using a Micromass Z-spray atmospheric pressure ionization (API) source equipped with a quadrupole and time-of-flight analyzer. Two kinds of capillaries were coupled to the ESI source: a borosilicate nanovial (Micromass) and an LC system combined with a C18 column (0.1 × 250 mm; GL Sciences, Tokyo, Japan). In the former, 1000 V was applied to the nanovial to cause electrostatic nebulization. The MS scan was acquired in the mass range m/z 400−2000, and then MS/MS analysis was performed using collision-induced dissociation (CID) with relative collision energies from 25% to 40%. The LC system used buffers A (1% FA/0.1% TFA in water) and B (1% FA/0.1% TFA in ACN). LC was performed with 5−60% buffer B over 55 min at a flow rate of 150 nL/min. The LC spectra were analyzed using Ultichrom Software (LC Packings, Amsterdam, The Netherlands). For LC-ESI-Q-TOF MS, the capillary voltage was set to 3900 V. The MS and MS/MS spectra were analyzed using Masslynx 3.5 software (Micromass). The MS and MS/MS spectra were used for the peptide mass fingerprint and amino acid sequencing, respectively.

Determining the Disulfide Bond Pattern of EDGP. Native EDGP (20 μg) was denatured for 1 h at 37 °C in 10 μL of 50 mM sodium phosphate buffer containing 8 M urea, pH

6.0. To this solution was added 2 μg of chymotrypsin, resolved in the same buffer (30 μL), and the resultant solution was incubated at 37 °C for 18 h. To prevent exchange of the disulfide bonds, NEM (final concentration 1 mM) was added to the reaction solution. The resultant digest was separated into two equal volumes, one of which was reduced completely with 10 mM DTT for 30 min at 37 °C. The volumes were desalted, concentrated using a ZipTip$_{\mu-C18}$ (Micromass), and then loaded into a borosilicate nanovial for ESI-Q-TOF MS analysis. In addition, they were subjected to LC-ESI-Q-TOF MS as described above.

To identify the disulfide bond pattern in the Cys-rich region (Figure 3), EDGP (150 μg) was denatured and digested with 15 μg of trypsin under the same conditions used for the chymotryptic digestion described above. These tryptic peptides were separated with a C4 column coupled to RP-HPLC from 13% to 23% buffer B over 20 min. All of the fractions were checked using MALDI-TOF MS, and a peptide with *m*/*z* 7600 was chosen for N-terminal sequencing by Edman degradation (Applied Biosystems, Foster, CA) to confirm whether it was the peptide containing the Cys-rich region. The corresponding fraction was lyophilized and resuspended in 10 μL of 100 mM citrate−phosphate buffer, pH 5.0. To the solution was added glycopeptidase A (0.2 milliunits), and the resultant solution was incubated for 18 h at 37 °C. The resultant digest was separated with a C18 column (1.0 × 100 mm; Nomura Chemical, Seto, Japan) coupled to an RP-HPLC with 13−23% buffer B over 20 min. Then, the deglycosylated peptide was collected and lyophilized. Subsequently, it was dissolved in 20 μL of 100 mM NaH_2PO_4 (pH 3.0) and digested with 2 μg of pepsin for 4 h at 37 °C, and 1 μL of the solution was analyzed directly using LC-ESI-Q-TOF MS, as described above. Another 1 μL was treated with TCEP (final concentration 1 mM) for 3 min at 37 °C for partial reduction of disulfide bonds and then subjected to LC-ESI-Q-TOF MS analysis. The remaining solution was incubated for a further 20 h. Then, 1 μL of the digest solution was analyzed using LC-ESI-Q-TOF MS. The remaining solution (14 μL) was mixed with TCEP (final concentration 1 mM) at 37 °C, and 1 μL was removed at 20 s intervals and mixed with NEM (final concentration 5 mM). Then, the mixture was incubated for 30 min at 37 °C and subjected to LC-ESI-Q-TOF MS analysis.

N-Terminal Modification. EDGP (10 μg) was denatured as described above. Before proteolytic digestion, the urea concentration in the protein sample was reduced to 2 M for chymotrypsin or trypsin or to 4 M for *S. aureus* V8 protease. A protease to protein molar ratio of 1:50 was used, and the solution was incubated for 6 h at 37 °C. The resultant peptides were analyzed using MALDI-TOF MS and ESI-Q-TOF MS.

Confirmation of the Putative Glycosylation Sites. The peptide containing the Cys-rich region (Cys^{84}−Arg^{147}) was isolated, as described above, and then digested with pepsin for 2 h. The resultant peptides were separated with a C4 column coupled to an RP-HPLC using 10−25% buffer B over 30 min and analyzed using MALDI-TOF MS. Then, they were deglycosylated with glycopeptidase A under the conditions described above. These treated peptides were desalted and concentrated with a ZipTip$_{\mu-C18}$ for MALDI-TOF MS analysis.

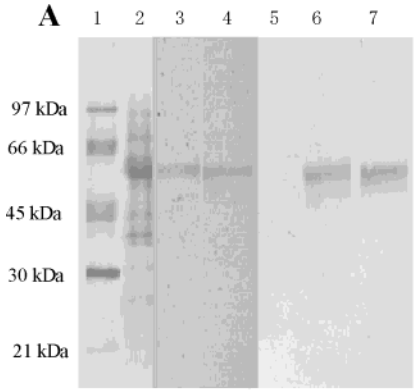

B

Frag #	Observed Mass (*m*/*z*)	Expected Mass (*m*/*z*)
T3	1609.75	1609.82
T4	1568.79	1568.86
T5	2348.21	2348.11
T8	670.42	670.43
T9	2609.05	2609.35
T11	1513.81	1513.95
T15	3401.68	3401.74
T19	1841.89	1841.99
T23*	2127. 96	2128.02
T25	2513.17	2513.31
T26	1093.55	1093.61

FIGURE 1: Identification of the 4-kDa peptide-binding protein. The eluent from the NTA sensor chip immobilized 4-kDa peptide was subjected to SDS−PAGE followed by western blotting (A, lanes 5−7) or MALDI-TOF MS (B) analysis. (A) Lanes 1 and 5, low molecular markers; lane 2, proteins from the carrot suspension culture medium; lanes 3 and 6, purified EDGP; lanes 4 and 7, the eluent from the 4-kDa peptide immobilized flow cell. (B) The observed masses were subjected to the protein database (http://prospector.ucsf.edu) for MS-Fit search, and the matched ones were listed. The asterisk (*) indicates that the Cys residue in the T23 peptide was modified with acrylamide during SDS−PAGE.

Another study to confirm the occupancy of the putative glycosylation sites in EDGP was also performed. In brief, EDGP (40 μg) was reduced, labeled with IAA, and then digested with trypsin at an enzyme:substrate molar ratio of 1:50 in 50 mM Tris-HCl buffer (pH 8.0) for 12 h at 37 °C. The digest was separated with a C4 column coupled to RP-HPLC using 5−50% buffer B over 90 min. The resultant fractions were blotted onto a PVDF membrane, and then the glycopeptides were identified using a glycoprotein detection kit (ECL kit; Amersham Biosciences), according to the manufacturer's instructions. Subsequently, the corresponding fractions were collected and analyzed using LC-ESI-Q-TOF MS.

RESULTS

Identifying the 4-kDa Peptide-Binding Protein in Carrot Callus Suspension Culture Medium. The proteins obtained from 3-week-old carrot callus suspension culture medium were subjected to SPR analysis. In the western blotting analysis, the eluent from the 4-kDa peptide immobilized target cell cross-reacted with anti-EDGP antibody (Figure 1A), suggesting that the binding protein was EDGP. Then, the protein was excised from the SDS−PAGE gel for in-gel digestion and analyzed using MALDI-TOF MS. The resultant mass fingerprint was compared with a database to identify

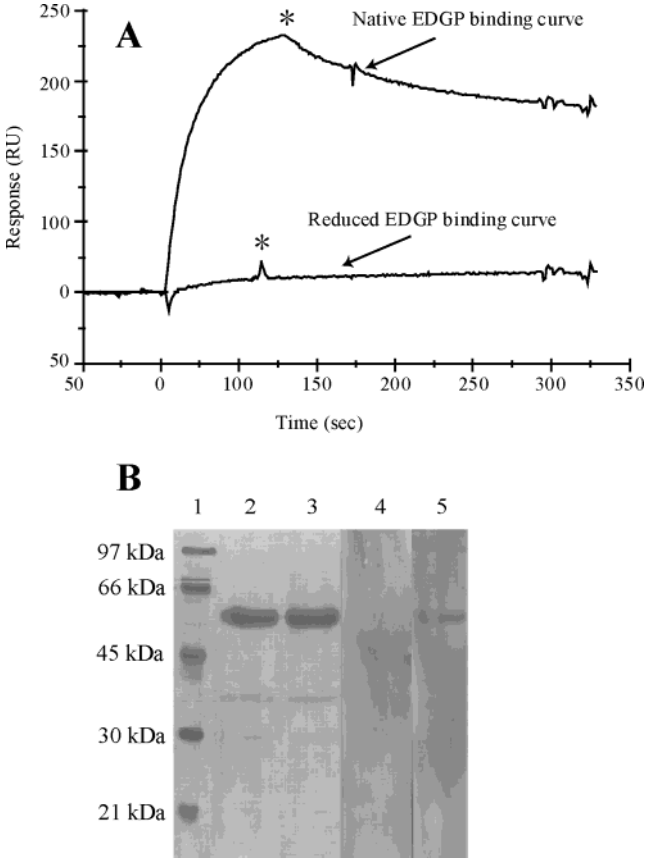

FIGURE 2: Effect of EDGP conformation on binding with the 4-kDa peptide. (A) Native and reduced EDGP binding means that EDGP binds to the His-tagged 4-kDa peptide on the target flow cell. All binding curves were corrected for background and bulk refractive index contribution by subtraction of the reference flow cell. Phases before the asterisk (*) represent the association sensorgrams; phases after the asterisk represent the dissociation sensorgrams. (B) EDGP was reduced and subjected to SDS−PAGE (lanes 1−3) followed by ligand blotting (lanes 4 and 5). Lane 1, low molecular marker; lanes 2 and 3, reduced EDGP; lane 4, EDGP was incubated directly with anti-4-kDa peptide antiserum (negative control); lane 5, EDGP was incubated with the wild-type 4-kDa peptide and then reacted with anti-4-kDa peptide antiserum.

the protein using MS-Fit (http://prospector.ucsf.edu). This protein was EDGP (Figure 1B).

Effect of EDGP Conformation on Binding with the 4-kDa Peptide. EDGP was applied to an SPR system with an NTA sensor chip immobilized His-tagged 4-kDa peptide. As shown in Figure 2A, native EDGP bound to the 4-kDa peptide with a strength exceeding 170 response units (RU), while reduction of the disulfide bonds in EDGP decreased the binding activity 20-fold. This difference demonstrates that the structure maintained by the disulfide bonds is very important for binding activity. In addition, the reduced EDGP was subjected to ligand blotting using the wild-type 4-kDa peptide. The reduced EDGP had weak binding activity (Figure 2B), suggesting that the 4-kDa peptide recognizes binding site(s) in the primary structure of EDGP.

Determining the Disulfide Bond Pattern of EDGP. EDGP was digested with chymotrypsin, and the resultant digest was divided to two volumes: one was applied to ESI-Q-TOF MS coupled with a borosilicate nanovial, and the other was reduced with DTT followed by MS analysis as described in Experimental Procedures. By comparison of the difference between the mass fingerprints from the nonreduced and reduced digests, peptide ions that were present only in the nonreduced digest spectrum were chosen for MS/MS sequencing. The results were as follows (all of the residue numbers used in this paper refer to the position in the full-length EDGP shown in Figure 9A).

(A) Cys^{70}−Cys^{158}. A zoomed MS scan (Figure 4A) showed that a doubly charged ion at *m*/*z* 972.53 ($[M + H]^+$ = 1944.06) was only present in the nonreduced digest spectrum, suggesting that the peptide(s) contained disulfide bond(s). The corresponding MS/MS analysis showed that the doubly charged ion (Figure 4A) contained two peptide ions: Leu^{66}−Tyr^{74} (b ions at *m*/*z* 300.19, 399.30, and 514.39; y ions at *m*/*z* 296.14; peptide mass, *m*/*z* 1155.25) and Ser^{157}−Leu^{164} (y ions at *m*/*z* 245.41, 530.41, and 601.45; peptide mass, *m*/*z* 790.93). The ion observed at *m*/*z* 1944.06 in the MS scan has the same mass as that of these two peptides minus the mass of two protons, which are lost during disulfide bond formation. A fragment ion of the dipeptide linked by the disulfide bond was also visualized at *m*/*z* 1414.49 in the MS/MS spectrum. Since only two Cys residues were present, the dipeptide must be linked by the disulfide bond between Cys^{70} and Cys^{158}. This was confirmed by on-target reduction followed by MALDI-TOF MS using a method described previously (*17*) (data not shown).

(B) Cys^{332}−Cys^{378}. Another zoomed MS scan (Figure 4B) showed that a doubly charged ion at *m*/*z* 642.37 ($[M + H]^+$ = 1283.74) was only present in the nonreduced digest spectrum, suggesting that the peptide(s) include(s) disulfide bond(s). The resultant MS/MS analysis (Figure 4B) only confirmed the peptide Ile^{372}−Leu^{379} (b ions at *m*/*z* 228.09, 343.11, 457.27, and 655.40). Therefore, we attempted to link all possible chymotryptic peptides containing Cys residues with the identified peptide, and the peptide Gly^{330}−Phe^{333} connected with the peptide Ile^{372}−Leu^{379} by a disulfide bond matched the observed mass (*m*/*z* 1283.74). Since only two Cys residues were present in the dipeptide, they must be linked by the disulfide bond between Cys^{332} and Cys^{378}. Moreover, dominant ions of the linked dipeptide fragments were visualized at *m*/*z* 501.25, 629.28, and 728.39 in the MS/MS spectrum, which provided further support for this conclusion.

Using a borosilicate nanovial coupled with ESI-Q-TOF MS, the disulfide bonds Cys^{70}−Cys^{158} and Cys^{332}−Cys^{378} were confirmed. Unfortunately, using this method, the other disulfide bonds could not be identified. There are two possible reasons for this: a complex MS/MS spectrum might result from two peptides with the same mass ($[M + 2H]^{2+}$ = 702.30), or the chymotryptic cleavage sites might be near the glycosylation sites, reducing the proteolytic ability and intensity of the resultant peptide in the mass spectrum. Hence, these ions would be difficult to sequence when mixed among ions with strong intensity. Due to the unresolved bonds, the same digests were applied to LC-ESI-Q-TOF MS.

(C) Cys^{84}−Cys^{89}. Two doubly charged ions at *m*/*z* 702.30 ($[M + H]^+$ = 1403.60) in the MS scan were separated using the LC system followed by MS/MS sequencing. One of the MS/MS spectra (Figure 5A) was verified to be from the peptide Arg^{80}−Leu^{91} (b ions at *m*/*z* 254.17, 353.25, and 509.35; peptide mass, *m*/*z* 1405.60). The observed mass was 2 Da less than that calculated from the amino acid sequence of the peptide, suggesting that Cys^{84} and Cys^{89} formed a disulfide bond. In addition, some ions in the MS/MS

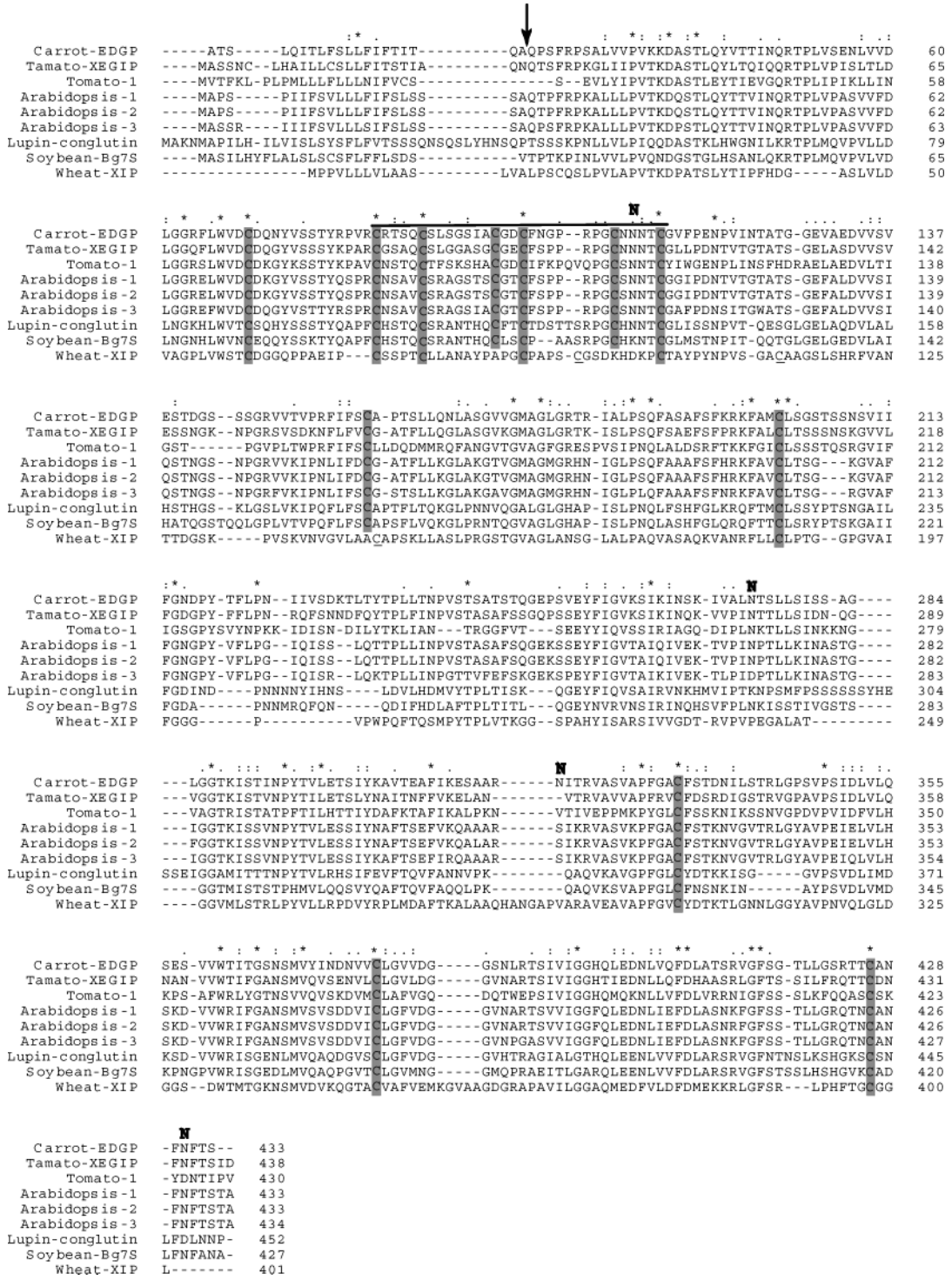

FIGURE 3: Alignment of the amino acid sequences of EDGP homologues. Clustal X (version 1.8) (http://bioinformatics.ubc.ca/resources/tools) was used to align the multiple amino acid sequences. Conserved Cys residues are highlighted, and putative glycosylation sites are labeled with N. The cleavage site of the signal peptide in EDGP is marked with an arrow. Unconserved Cys residues in wheat XIP are underlined. The line above the EDGP sequence indicates the Cys-rich region. The accession number and homology (percent amino acid sequence to identity to EDGP) for each gene and protein are as follows: D14550 (carrot-EDGP, 100%); AY155579 (tomato-XEGIP, 64%); TC116578 (tomato-1, 39%); AAC72119 (Arabidopsis-1, 39%); AAM61574 (Arabidopsis-2, 38%); AAC72120 (Arabidopsis-3, 38%); CAC16394 (Lupin-conglutin, 39%); AAB03390 (Soybean-Bg7S, 33%); AJ438880 (Wheat-XIP, 25%).

spectrum (such as the b ions at *m*/*z* 1168.57 and 1256.62 and y ions at *m*/*z* 895.4, 1051.95, 1150.60, and 1247.7) also differed from the theoretical values by 2 Da, confirming the disulfide bond between Cys^{84} and Cys^{89}.

(D) Cys^{201}−Cys^{426}. A doubly charged ion at *m*/*z* 695.83 ($[M + H]^+ = 1390.66$) with weak intensity was only present in the nonreduced MS spectrum. The resultant MS/MS spectrum (Figure 5B) showed that this ion contained two peptide ions: Ala^{199}−Leu^{202} (b ion at *m*/*z* 203.69; peptide mass, *m*/*z* 436.60) and Gly^{421}−Phe^{429} (b ions at *m*/*z* 301.17, 402.21, and 503.27; y ion at *m*/*z* 349.25; peptide mass, *m*/*z* 956.05). Linking the two peptides via a disulfide bond (Cys^{201}−Cys^{426}) generates a dipeptide with a mass of 1390.65, which is in good agreement with the measured mass

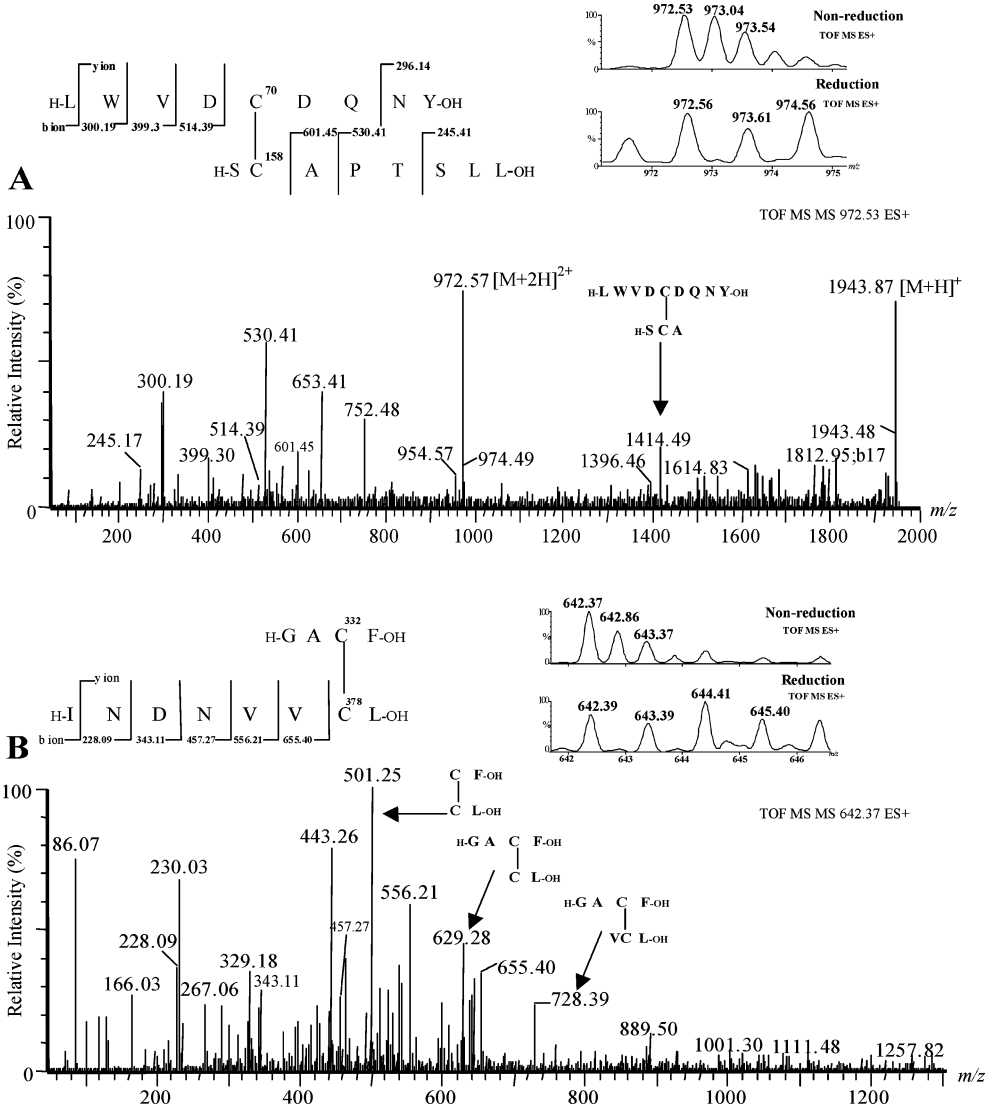

FIGURE 4: Identification of disulfide bonds Cys[70]−Cys[158] and Cys[332]−Cys[378]. Nonreduced and reduced chymotryptic peptides of EDGP were analyzed with nanovial ESI-Q-TOF MS. By comparison of the MS spectra before and after reduction, possible ions generated from disulfide-linked peptides were for MS/MS sequencing. (A) A doubly charged ion at *m*/*z* 972.53 in a zoomed MS spectrum (shown in right corner, nonreduction) was chosen for MS/MS analysis. The corresponding MS/MS spectrum contained fragment ions produced from Leu[66]−Tyr[74] and Ser[157]−Leu[164], confirming the linkage between Cys[70] and Cys[158]. (B) Another doubly charged ion at *m*/*z* 642.3 in a zoomed MS scan (shown in right corner, nonreduction) was selected for MS/MS analysis. The MS/MS spectrum only confirmed the peptide Ile[372]−Leu[379]; therefore, a possible peptide Gly[330]−Phe[333] was linked with the identified peptide. Some ions generated from fragments of the linked dipeptide were found, such as *m*/*z* 501.25, 629.28, and 728.39. These confirmed disulfide bond Cys[332]−Cys[378].

of 1390.66. Furthermore, some fragment ions of the two peptides linked by the disulfide bond were found in the MS/MS spectrum, such as *m*/*z* 909.44 and 1171.46. These data verified the disulfide bond between Cys[201] and Cys[426].

Using chymotryptic cleavage followed by an MS scan and MS/MS sequencing, we confirmed the four disulfide bonds described above. However, the remaining four Cys residues (Cys[97], Cys[100], Cys[108], and Cys[113]) were located in a Cys-rich region (Cys[84]−Cys[113]) with two Pro residues and a glycosylation site (Asn[110] was converted to Asp[110] during deglycosylation; refer to Figure 8A), which prevented tryptic or chymotryptic cleavage. Therefore, the peptide (Cys[84]−Arg[147]) containing the Cys-rich region was first separated from the tryptic digest, and then a protease (pepsin) with low substrate specificity was used to analyze the disulfide bonds. The results are listed below.

(E) Cys[97]−Cys[113]. The Cys-rich peptide was digested with pepsin for 4 h. After treating it with TCEP for 3 min, a doubly charged peptide at *m*/*z* 1130.37 ([M + H]$^+$ = 2259.74) was only found in a zoomed nonreduced digest MS spectrum, suggesting that the peptide(s) contain(s) disulfide bridge(s). The corresponding MS/MS spectrum (Figure 6A) showed that two peptide ions were present: Ser[92]−Asp[99] (b ions at *m*/*z* 232.11 and 345.29; peptide mass, *m*/*z* 708.75) and Cys[100]−Gly[114] (b ions at *m*/*z* 251.08, 365.13, 422.12, etc.; peptide mass, *m*/*z* 1554.70). The MS/MS analysis of peptide Cys[100]−Gly[114] produced a spectrum with dominant fragments at *m*/*z* 251.08, 365.13, 422.12, 518.18, 675.27, 828.34, and 933.43, which confirmed that Cys[100] and Cys[108] were reduced. Evidence for a disulfide linkage between Cys[97] and Cys[113] came from the presence of ions in the MS/MS spectrum at *m*/*z* 379.08, 450.12, and 621.14, which corresponded with the fragments of the dipeptide linked by the disulfide bond. Cleavage of pepsin is specific at pH 1.3; under these conditions, pepsin preferentially cleaves the C-terminal side of Phe, Leu, and Glu. Since this

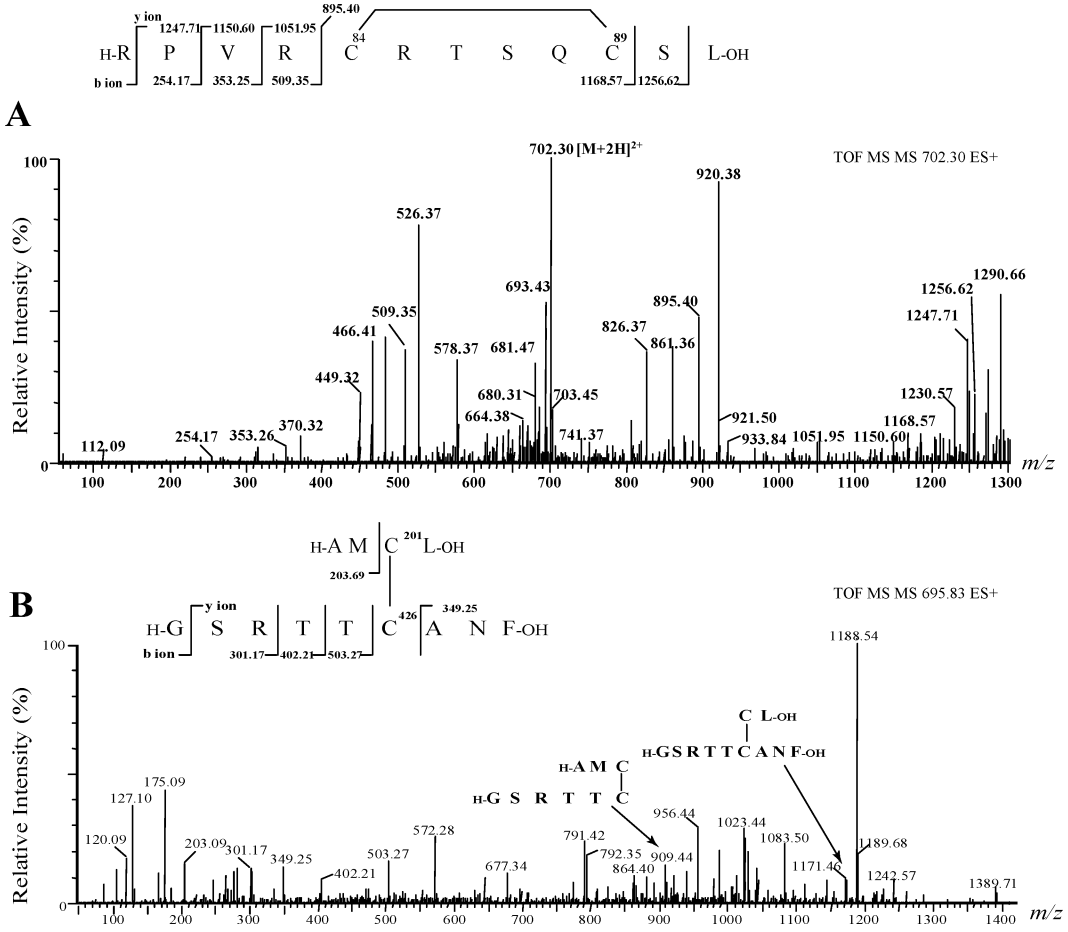

FIGURE 5: Identification of disulfide bonds Cys[84]−Cys[89] and Cys[201]−Cys[426]. The reduced and nonreduced chymotryptic digests were analyzed with LC-ESI-Q-TOF MS. (A) MS/MS analysis of a doubly charged ion at *m*/*z* 702.30 confirmed a peptide Arg[80]−Leu[91]. The molecular mass of this peptide was different from the observed one by 2 Da, and some ions (b ions at *m*/*z* 1168.57 and 1256.62; y ions at *m*/*z* 895.40, 1051.95, 1150.60, and 1247.71) also showed the same difference. These results confirmed the disulfide bond Cys[84]−Cys[89]. (B) MS/MS analysis of a doubly charged ion at *m*/*z* 695.83 confirmed two peptides: Ala[199]−Leu[202] and Gly[421]−Phe[429]. The mass of the dipeptide linked by a disulfide bond was in agreement with the observed one. Moreover, ions produced from fragments of the linked dipeptide were found, such as *m*/*z* 909.44 and 1171.46. These results confirmed that a disulfide bond formed between Cys[201] and Cys[426].

specificity is lost at pH >2 (*25*), it is possible that pepsin cleavage also happens at the C-terminal side of Gly and Pro residues, as shown in these experiments.

(F) Cys[100]−Cys[108]. The peptide containing the Cys-rich region was incubated with pepsin for up to 24 h. This digest was mixed with TCEP, and 1 μL of the mixture was transferred to *N*-ethylmaleimide (NEM) solution at 20 s intervals and subjected to LC-ESI-Q-TOF MS. A doubly charged ion at *m*/*z* 1007.81 ($[M + H]^+ = 2014.62$) was only present in the reduced digest MS spectrum (Figure 6B), suggesting that this peptide is reduced and labeled with NEM. By calibrating all the possible linkages via disulfide bonds, it was found that two peptides (Cys[97]−Phe[101] and Pro[106]−Pro[117]) might be connected by a disulfide bond. Linking the two peptides ($[M + H]^+ = 543.75$ and 1223.48, respectively) via a disulfide bond generated a dipeptide with a mass of 1767.23, which differed from the observed mass by 250 Da. This difference was explained by the addition of two molecules of NEM to these two peptides (each NEM increases the mass by 125 Da). Ions at *m*/*z* 286.08 and 401.10 in the MS/MS spectrum (Figure 6B) suggested that Cys[97] was reduced and alkylated by NEM. Since Cys[97]−Cys[113] was confirmed, the other alkylated residue must be Cys[113]. Furthermore, some ions generated from the fragments of the linked dipeptide (*m*/*z* 825.35, 883.33, 940.37, 1055.40, and 1900.07) in the MS/MS spectrum confirmed that Cys[100] and Cys[108] were connected by a disulfide bond.

N-Terminal Modification. Satoh et al. (*1*) suggested that a signal peptide is involved in the EDGP precursor. When subjected to Edman degradation sequencing, EDGP could not be sequenced, indicating that it is an N-terminally blocked protein. In this study, after digestion with *S. aureus* V8 protease followed by MALDI-TOF MS, a possible N-terminal peptide was visualized at a mass of 1750.80 (Figure 7A), which differed from the theoretical value (*m*/*z* 1767.80) by 17 Da. The same result was obtained with tryptic digestion (Figure 7B), indicating that the N-terminal Gln residue is cyclized to pyroglutamic acid, which results in the 17-Da decrease in the N-terminal peptide. Moreover, the MS/MS analysis of a chymotryptic peptide with a doubly charged ion at *m*/*z* 493.29 ($[M + H]^+ = 985.58$) produced a series of b ions, such as *m*/*z* 209.11, 296.13, 433.24, and 599.32, which were all consistent with the theoretical masses minus 17 Da (Figure 7C). The cyclized form of the Gln residue makes the amino-terminal group resistant to Edman sequencing.

Occupancy of N-Linked Glycosylation Sites. On digestion with trypsin and pepsin, ions generated from two peptides (Cys[84]−Glu[132] and Cys[84]−Asp[133]) were observed at *m*/*z* 6135.54 and 6250.83 in the MALDI-TOF MS spectrum

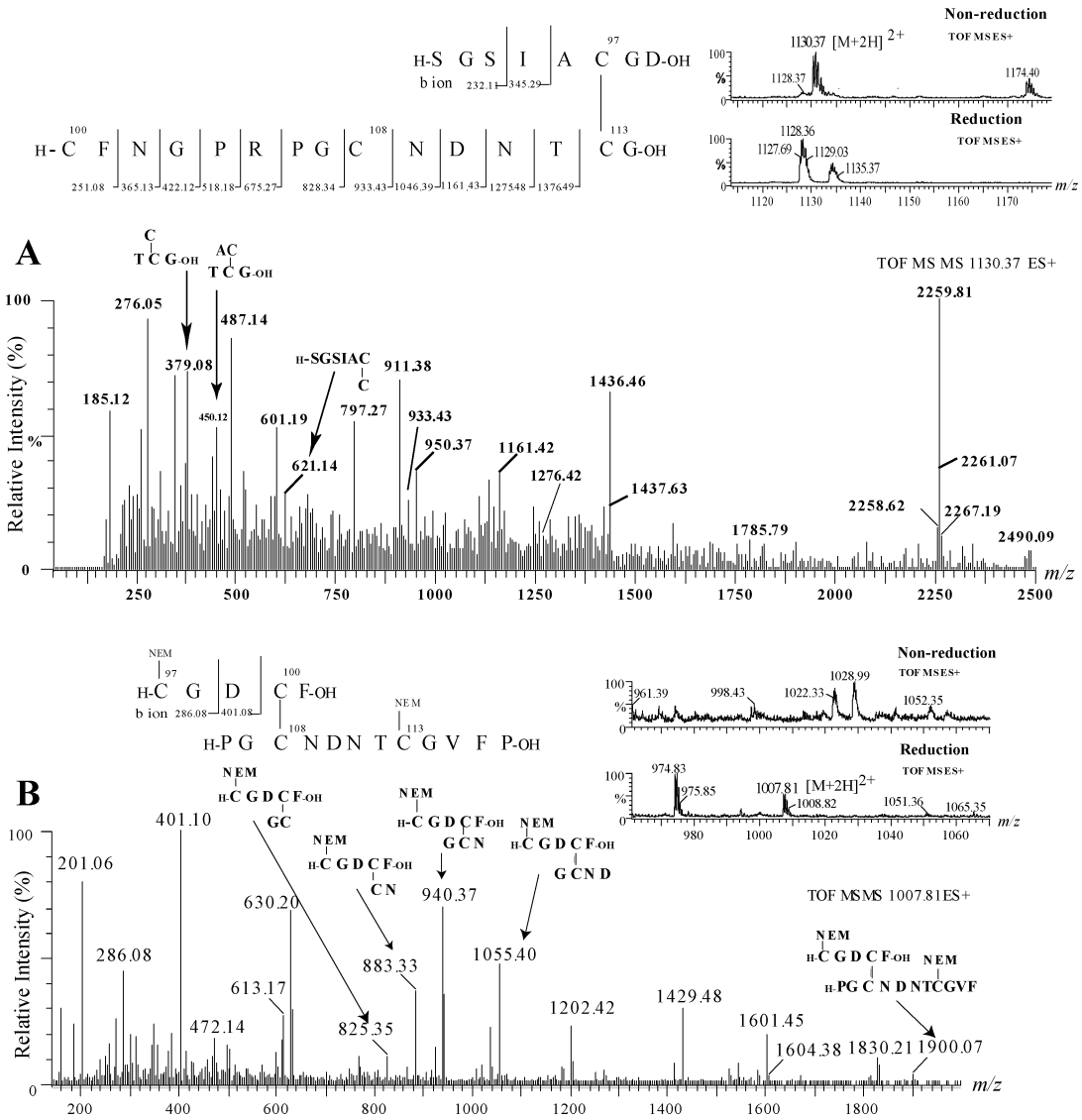

FIGURE 6: Identification of disulfide bonds Cys^{97}−Cys^{113} and Cys^{100}−Cys^{108}. A peptide containing the Cys-rich region was selected and subjected to pepsin digestion (for details, see Experimental Procedures). (A) The peptide was digested with pepsin for 4 h followed by partial reduction. By comparison of the MS spectra before and after reduction, a doubly charged ion at *m*/*z* 1131.37 (shown in right corner, nonreduction) was selected for MS/MS analysis. The resultant spectrum confirmed two peptides: Ser^{92}−Asp^{99} and Cys^{100}−Gly^{114}. Some b ions generated from the peptide Cys^{100}−Gly^{114} showed that Cys^{100} and Cys^{108} residues were free. Ions produced from the fragments of the dipeptide linked via a disulfide bond were found, such as *m*/*z* 379.08, 450.12, and 621.14. These results confirmed the disulfide bond Cys^{97}−Cys^{113}. (B) The same peptide was digested with pepsin for up to 24 h followed by partial reduction and alkylation. A doubly charged ion at *m*/*z* 1007.81 was only present in the reduced digest MS spectrum (shown in right corner, reduction), suggesting that this peptide should be labeled with NEM. Linking two possible peptides (Cys^{97}−Phe^{101} and Pro^{106}−Pro^{117}) via a disulfide bond generated a dipeptide, whose mass was different from the observed one by 250 Da (equal to the total mass of two NEM molecules). Ions at *m*/*z* 286.08 and 401.10 suggested that Cys^{97} alkylated with NEM. Since Cys^{97}−Cys^{113} had been confirmed, another alkylated residue must be Cys^{113}. Furthermore, some ions generated from the fragments of the linked dipeptide (*m*/*z* 825.35, 883.33, 940.37, 1055.40, and 1900.07) confirmed that Cys^{100} and Cys^{108} were connected for a disulfide bond.

(Figure 8A). After deglycosylation with glycopeptidase A, the masses of the two ions were reduced to *m*/*z* 4968.44 and 5083.61. A mass difference of 1167 Da was observed. During deglycosylation, the glycosylated Asn^{110} was converted into Asp^{110}, which increases the masses of these deglycosylated peptides by 1 Da. Therefore, the putative glycosylation site (N^{110}NT) is occupied by a glycan with a mass of 1168 (±3) (Figure 8A). Furthermore, MS/MS sequencing of the fragments from the Cys-rich region (Figure 6) confirmed that Asn^{110} was converted into Asp^{110}.

Since the masses of the other glycans are unknown, each glycopeptide must be determined with an MS scan followed by N-terminus sequencing, which is time-consuming. Carr et al. (*18*) reported that a glycopeptide could be determined using marker ions in the MS/MS spectrum, such as *m*/*z* 163 [protonated hexose residue (Hex)], *m*/*z* 204 [protonated *N*-acetylhexosamine residue (HexNAc)], *m*/*z* 366 (protonated Hex-HexNAc), or *m*/*z* 407 [protonated $(HexNAc)_2$]. There is no O-linked glycosylation in EDGP (*15*); hence, HexNAc should be referred to *N*-acetylglucosamine (GlcNAc). Using a glycoprotein detection kit, some possible tryptic glycopeptides were identified (Figure 8B, spots 1, 2, 3, and 5), and these were then subjected to LC-ESI-Q-TOF MS. MS/MS analysis of a doubly charged ion at *m*/*z* 1057.91 ($[M + H]^+ = 2114.82$) produced a series of b ions at *m*/*z* 213.15, 284.14, 397.10, 511.30, 612.35, 812.37, and 943.33, which

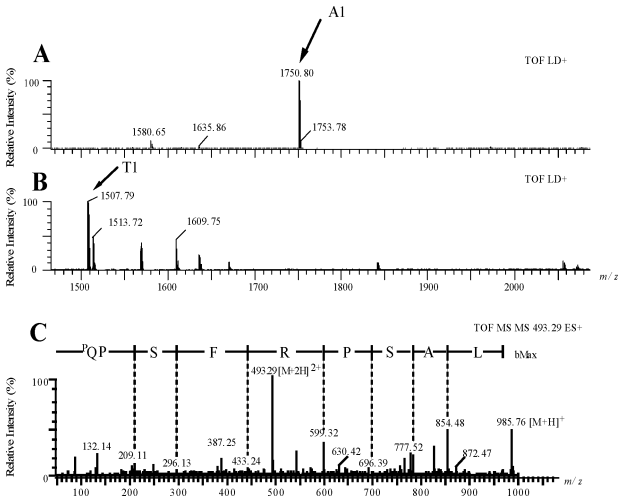

FIGURE 7: N-Terminal modification of EDGP. MALDI-TOF MS spectra were obtained from *S. aureus* V8 protease (A) or trypsin digestion (B). The molecular mass of first peptide (A1 or T1) was less than the theoretical one by 17 Da. In addition to this, MS/MS analysis of a chymotryptic peptide with a doubly charged ion at *m*/*z* 493.3 confirmed that the N-terminal glutamine was cyclized to pyroglutamic acid, which leads to a 17-Da decrease.

corresponded to the peptide $Ile^{270}-Leu^{278}$ ($[M + H]^+ = 943.15$). The mass of the peptide differed from the observed mass by 1171.67 Da, which was explained by glycosylation at the Asn^{274} ($N^{274}TS$) residue, and the mass of the glycan was *m*/*z* 1171.67. The ions at *m*/*z* 163.10, 204.04, 366.10, and 407.11 in the MS/MS spectrum were glycan marker ions, as described above, which provided further evidence of glycosylation. Under MS/MS sequencing conditions, separation of the components of the glycan was easier than peptide bond cleavage, which resulted in a high intensity of glycan marker ions in the MS/MS spectrum. Separating the glycan from the glycosylated Asn residue requires less energy than cleaving a peptide bond; hence, the native Asn^{274} residue was found in the MS/MS spectrum. The peptide was cleaved at the C-terminal side of Leu^{278}; this might have resulted from a trace of chymotrypsin in the trypsin and the long incubation.

Similarly, another MS/MS analysis of a doubly charged ion at *m*/*z* 1167.82 ($[M + H]^+ = 2334.64$) produced a series of b ions at *m*/*z* 203.10, 364.30, 435.15, 549.07, 696.23, 957.33, and 1058.18, which corresponded to the peptide $Thr^{424}-Ser^{433}$ (containing an alkylated Cys^{426} residue) (Figure 8D). The theoretical mass of this peptide differed from the observed one by 1171.45 Da, meaning that Asn^{430} ($N^{430}FT$) was also glycosylated with a glycan at *m*/*z* 1171.45. Glycan marker ions such as *m*/*z* 163.04 and 204.05 in the MS/MS spectrum provided further evidence of glycosylation.

MS/MS analysis of a doubly charged ion at *m*/*z* 1104.35 ($[M + H]^+ = 2207.70$) produced some glycan marker ions, as described above, implying that the corresponding peptide is glycosylated. Some fragment ions (data not shown) suggested that the peptide was amino acids $Glu^{314}-Arg^{322}$ ($[M + H]^+ = 1036.52$), which contain a putative glycosylation site ($N^{319}IT$) and differed from the observed mass by 1171.18. The result suggested that the Asn^{319} residue was also glycosylated.

EDGP contains two isoforms with very similar amino acid compositions but different p*I* values (8.8 and 9.5), in which the polypeptide (p*I* 9.5) was the dominant form (*15*). Using nanovial ESI-Q-TOF MS, the mass of EDGP with a p*I* value at 9.5 was determined to be *m*/*z* 48282 (±5) (data not shown), whereas the theoretical mass based on the amino acid sequence of mature EDGP is 43601 (including disulfide bonds and N-terminal modification). The difference is 4681 (±5), which is consistent with the total mass of the four glycans (1168 + 1171 + 1171 + 1171 = 4681). Hence, the posttranslational modifications of EDGP (p*I* 9.5) involve only disulfide bonds, N-terminal modification, and glycosylation.

DISCUSSION

This study identified a 4-kDa peptide-binding protein in carrot callus suspension culture medium as an EDGP. However, the effect of the interaction between EDGP and the 4-kDa peptide on proliferation, differentiation, or stress response in carrot callus is not confirmed.

There are two possibilities. One is that EDGP is a hormone-receptor protein like the soybean 43-kDa protein, which means that a hormone peptide like the 4-kDa peptide might activate or stimulate the activity of EDGP, followed by a series of reactions such as phosphorylation, ultimately stimulating the proliferation of cultured carrot callus. The similarity in the ultrastructural localization, amino acid sequence, and some functions of the soybean 43-kDa protein and EDGP support this possibility. Nevertheless, the antisense 4-kDa peptide gene had no effect on the development of callus (*16*), indicating that the amino acid sequences of the 4-kDa peptides in soybean and carrot differ. There were also some differences between EDGP and the soybean 43-kDa protein; for example, EDGP was composed of single polypeptide (*15*), while the soybean 43-kDa protein was cleaved posttranslationally at the N-terminus of a Ser residue to generate α and β subunits (*8*). Gel filtration showed that EDGP was a monomer (data not shown), while the two soybean 43-kDa proteins formed a dimer that interacted with the 4-kDa peptide (*10*). Therefore, if EDGP is a hormone-receptor protein, the interaction mechanism differs from that in legumes. Moreover, EDGP is a hormone peptide carrier protein, which functions as an insulin-like growth factor (IGF) binding protein (IGFBP). An IGFBP can transport IGFs and prevent their degradation, limit their binding to IGF receptors, and modulate the actions of IGFs (*19*−*22*). Like IGFBPs (*23*), the appropriate tertiary structure of EDGP formed by disulfide bonds results in high affinity for the 4-kDa peptide, while the reduced form showed a low affinity (Figure 2). Until more is known about the functions of EDGP, the effect of this interaction cannot be confirmed.

All 12 Cys residues are conserved in the EDGP homologues, with the exception of the xylanase inhibitor protein (XIP) from wheat (Figure 3). In XIP, nine Cys residues are conserved, suggesting that they have a similar disulfide bone pattern. The peptide containing the Cys-rich region is also a hydrophobic proline-rich region, which might drive the peptide to form a hydrophobic patch. The interplay between bone morphogenetic protein (BMP) and its antagonist (Noggin) (*24*) shows that a hydrophobic side chain (a proline residue is thought to be a key determinant) from a flexible backbone segment of Noggin is first inserted into the hydrophobic pocket of BMP; then, complementary interactions occur between the two curved hydrophobic surfaces. By mimicking a similar interaction, the disulfide bonds

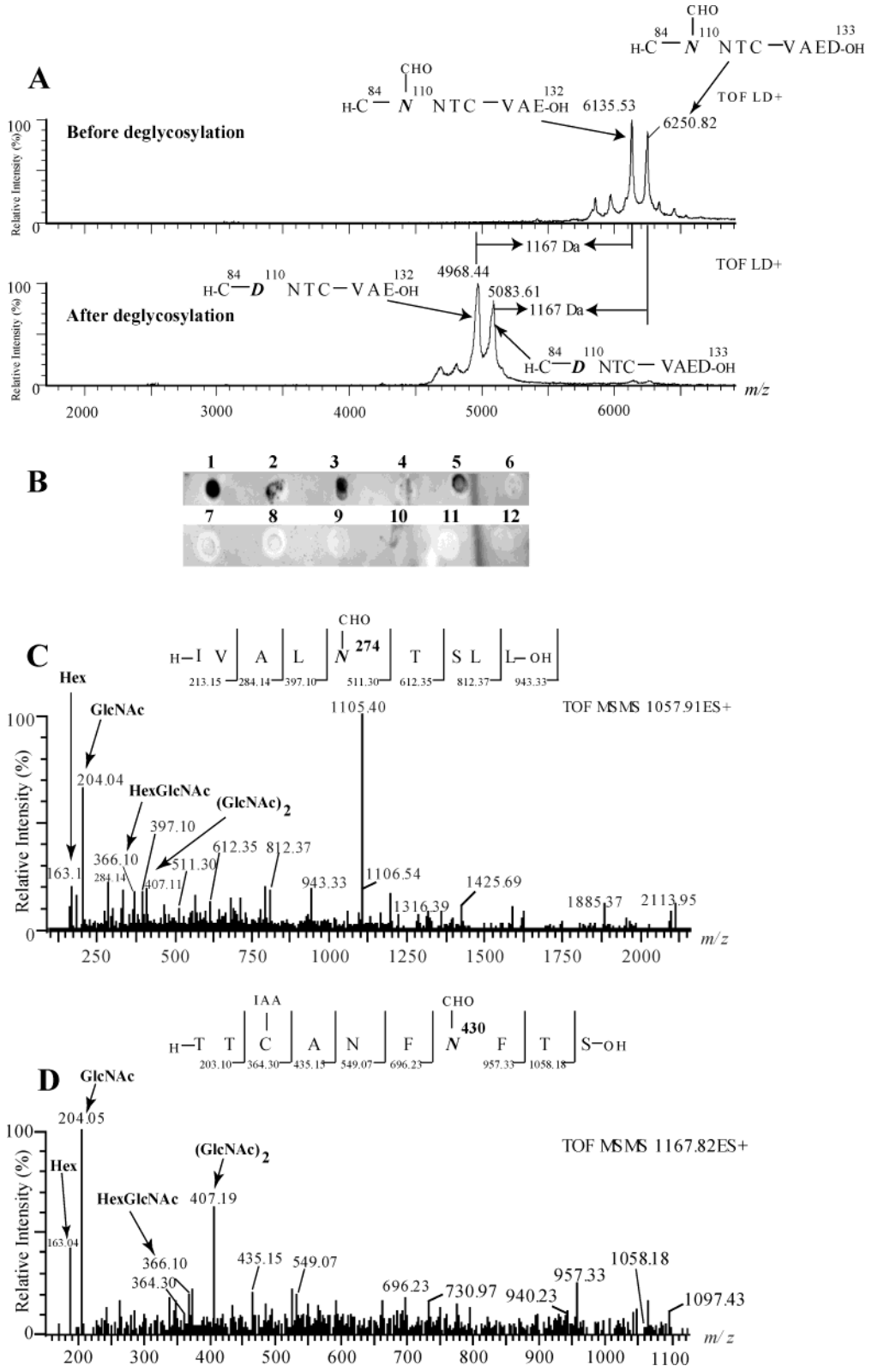

FIGURE 8: Occupancy of N-linked glycosylation sites. (A) Two fragments of EDGP ($Cys^{84}-E^{132}$ and $Cys^{84}-D^{133}$) were observed in the MALDI-TOF MS spectrum. After deglycosylation with glycopepsidase A, the masses of the two fragments were reduced by 1167 (±3) Da. During deglycosylation, the glycosylated Asn^{110} was converted into Asp^{110}, which increases the masses of these deglycosylated peptides by 1 Da. These results confirmed that the Asn^{110} residue was glycosylated by a glycan at *m*/*z* 1168 (±3). (B) A glycosylation detection kit was employed to find glycopeptides in the tryptic digest. Fractions 1, 2, 3, and 5 were subjected to MS/MS sequencing. (C) MS/MS analysis of a doubly charged ion at *m*/*z* 1057.91 confirmed the peptide $Ile^{270}-Leu^{278}$, whose mass was different from the observed one by 1171 Da. Combining the result of the glycan detection kit with glycan marker ions in the MS/MS spectrum, such as *m*/*z* 163.10, 204.04, 366.10, and 407.11, this peptide was confirmed as a glycopeptide, meaning that the Asn^{274} residue was glycosylated with a glycan of *m*/*z* 1171. (D) Similarly, MS/MS spectrum of a doubly charged ion at *m*/*z* 1167 confirmed that Asn^{430} was also glycosylated by a glycan of *m*/*z* 1171. In the peptide, the Cys^{426} residue was alkylated with IAA, which increased the mass of this peptide by 58 Da.

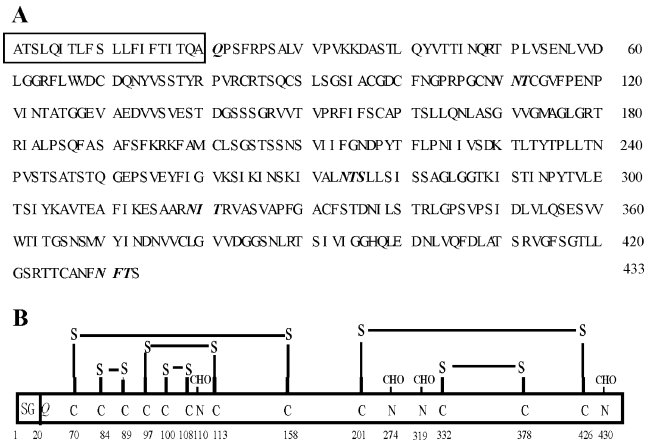

FIGURE 9: Amino acid sequence of EDGP and scheme of its posttranslational modification. (A) Amino acid sequence of EDGP deduced from its cDNA (GenBank accession number D14550). The signal peptide is boxed. The N-terminal glutamine and glycosylation sites are italicized. (B) Scheme of posttranslational modification of EDGP. SG = signal peptide; the connection lines = disulfide bonds; CHO = glycan group.

(Cys^{84}−Cys^{89}, Cys^{97}−Cys^{113}, and Cys^{100}−Cys^{108}) in EDGP should form a hydrophobic clip domain, and Pro^{104} or Pro^{106}, or both, is inserted into a hydrophobic pocket on the 4-kDa peptide formed by Ile^{25}, Val^{29}, Phe^{31}, and Ile^{33} (*10*, *16*). The proline residues are embedded in two disulfide bonds (Cys^{97}−Cys^{113} and Cys^{100}−Cys^{108}), which may serve to enhance the conformation suitable for interaction. Even when EDGP is reduced, specific binding based on the hydrophobicity of the Cys-rich region may also occur, which might explain why reduced EDGP binds to the 4-kDa peptide weakly (Figure 2C). A search of the Prosite database (http://cn.expasy.org/prosite) showed that the disulfide bond pattern in the Cys-rich region was similar to that of C-type lectin; however, EDGP lacks lectin activity (*15*). The fact that all of the Cys residues are conserved in EDGP and the soybean 43-kDa protein (Figure 3) suggests that they share a common disulfide bond pattern. Therefore, the α and β subunits of the soybean 43-kDa protein should be connected by a Cys^{185}−Cys^{394} disulfide bridge. Moreover, Qin et al. (*6*) showed that XEG can be inhibited by XEGIP and EDGP. These two proteins share 61% amino acid sequence identity, and all of their Cys residues are conserved. When EDGP was reduced and labeled with IAA, it no longer inhibited XEG (data not shown), suggesting that the tertiary structure maintained by the disulfide bridges is necessary for its physiological function.

The four putative glycosylation sites are fully occupied (Figure 8). We attempted to use PNGase F to deglycosylate both native and denatured EDGP. However, even when treated for a week, they were resistant to the enzyme, suggesting that all four N-linked GlcNAc groups are coupled to (α-1,6) fucose. Therefore, the glycopeptide was exposed to glycopeptidase A, which has a similar action to PNGase F but can remove N-linked GlcNAc coupled to (α-1,6) fucose. The glycan was removed (Figure 8A), providing further evidence for the possibility described above. By contrast, endoglycosidases F1, F2, and F3 were used in an attempt to deglycosylate native EDGP; however, none of them worked, even after a 4-day treatment. The resistance to glycosidase implies that glycosylation plays an important role in the function(s) of EDGP, such as in signal transduction, hormone peptide protection, or invader recognition. Satoh et al. (*15*) reported that the monosaccharide composition in EDGP glycans contains GlcNAc, mannose, glucose, xylose, and fucose. The glycans in EDGP have a similar mass of 1171. According to these data, we searched the monosaccharide composition in a database (http://kr.expasy.org/tools/glycomod/glycanmass.html). The result shows that the glycan may contain two GlcNAc groups (203.20 Da for each), a (α-1,6) fucose (146.14 Da) coupled to the N-linked GlcNAc group, three hexoses (mannose or glucose; 162.15 Da for each), and a xylose (132.12 Da). The mass of the glycan in EDGP is 1171 Da, which is consistent with the sum of the monosaccharides.

A database search using the ExPASy proteomic tools (http://us.expasy.org/tools/) found some putative modification motifs. EDGP has a small ubiquitin-related modifier (SUMO)−protein attachment site (ALVVPVK^{34}KDASTLQ) and 11 putative phosphorylation sites (eight of them from protein kinase C and three from casein kinase II). The putative motifs indicate that EDGP is a multifunction protein.

In conclusion, we identified the 4-kDa peptide-binding protein from carrot callus medium as an EDGP and determined its posttranslational modification, which involves disulfide bonds, N-terminal modification, and glycosylation (Figure 9B). This may provide a molecular basis for analyzing the functions of EDGP-like proteins.

ACKNOWLEDGMENT

We thank Dr. Hiroshi Kawasaki for technical assistance and helpful discussion. We also thank Miss Kazumi Fujimoto for preparing anti-EDGP antibody.

REFERENCES

1. Satoh, S., Sturm, A., Fujii, T., and Chrispeels, M. J. (1992) cDNA cloning of an extracellular dermal glycoprotein of carrot and its expression in response to wounding, *Planta 188*, 432−438.
2. Ditt, R. F., Nester, E. W., and Comai, L. (2001) Plant gene expression response to *Agrobacterium Tumefaciens*, *Proc. Natl. Acad. Sci. U.S.A. 98*, 10954−10959.
3. Kagawa, H., Yamauchi, F., and Hirano, H. (1987) Soybean basic 7S globulin represents a protein widely distributed in legume species, *FEBS Lett. 226*, 145−149.
4. Chung, P., Neumann, G. M., and Polya, G. M. (1997) Purification and characterization of basic proteins with in vitro antifungal activity from seeds of cotton, *Gossypium hirsutum*, *Plant Sci. 127*, 1−16.
5. Fierens, K., Brijs, K., Courtin, C., Gebruers, K., Goesaert, H., Raedschelders, G., Robben, J., Van Campehout, S., Volckaert, G., and Delcour, J. (2003) Molecular identification of wheat endoxylanase inhibitor TAXI-I1, member of a new class of plant proteins, *FEBS Lett. 540*, 259−263.
6. Qin, Q., Bergmann, C. W., Rose, J. K. C., Saladie, M., Kumar Kolli, V. S., Albersheim, P., Darvill, A. G., and York, W. S. (2003) Characterization of a tomato protein that inhibits a xyloglucan-specific endoglucanase, *Plant J. 34*, 327−338.
7. Watanabe, Y., Barbashov, S. F., Komatsu, S., Hemmings, A. M., Miyagi, M., Tsunasawa, S., and Hirano, H. (1994) A peptide that stimulates phosphorylation of the plant insulin-binding protein. Isolation, primary structure and cDNA cloning, *Eur. J. Biochem. 224*, 167−172.
8. Komatsu, S., and Hirano, H. (1991) Plant basic 7S globulin-like proteins have insulin and insuling-like growth factor binding activity, *FEBS Lett. 294*, 210−212.
9. Nishizawa, Satoshi, M., Yoshihiro, W., and Hisashi, H. (1994) Ultrastructural localization of the basic 7S globulin in soybean (*Glycine max*) cotyledons, *Plant Cell Physiol. 35*, 1079−1085.

10. Hanada, K., Nishiuchi, Y., and Hirano, H. (2003) Amino acid residues on the surface of soybean 4-kDa peptide involved in the interaction with its binding protein, *Eur. J. Biochem. 270*, 2583−2592.
11. Murashige, T., and Skoog, F. (1962) A revised medium for rapid growth and bioassays with tobacco tissue cluture, *Physiol. Plant 15*, 473−497.
12. Bradford, M. M. (1976) A rapid and sensitive method for the quantitation of microgram quantities of protein utilizing the principle of protein-dye binding, *Anal. Biochem. 72*, 248−254.
13. Hirano, H., and Watanabe, T. (1990) Microsequencing of proteins electrotransferred onto immobilizing matrices from polyacrylamide gel electrophoresis: application to an insoluble protein, *Electrophoresis 11*, 573−580.
14. Hellman, U., Wernstedt, C., Gonez, J., and Heldin, C. (1995) Improvement of an "In-Gel" digestion procedure for the micropreparation of internal protein fragments for amino acid sequencing, *Anal. Biochem. 224*, 451−455.
15. Satoh, S., and Fujii, T. (1988) Purification of GP57, and auxin-regulated extracellular glycoprotein of carrots, and its immunocytochemical localization in dermal tissues, *Planta 175*, 364−373.
16. Yamazaki, T., Takaoka, M., Katoh, E., Hanada, K., Sakita, M., Sakata, K., Nishiuchi, Y., and Hirano, H. (2003) A possible physiological function and the tertiary structure of a 4-kDa peptide in legumes, *Eur. J. Biochem. 270*, 1269−1276.
17. Mhatre, R., Woodard, J., and Zeng, C. (1999) Strategies for locating disulfide bonds in a monoclonal antibody via mass spectrometry, *Rapid Commun. Spectrom. 13*, 2503−2510.
18. Carr, S. A., Huddleston, M. J., and Bean, M. F. (1993) Selective identification and differentiation of *N*- and *O*-linked oligosaccharides in glycoproteins by liquid chromatography-mass spectrometry, *Protein Sci. 2*, 183−196.
19. Cohen, P., Peehl, D., Lamson, G., and Rosenfeld, R. (1991) Insulin-like growth factors (IGFs), IGF receptors, and IGF-binding proteins in primary cultures of prostate epithelial cells, *J. Clin. Endocrinol. Metab. 73*, 401−407.
20. Shimasaki, S., Shimonaka, M., Zhang, H., and Ling, N. (1991) Identification of five different insulin-like growth factor binding proteins (IGFBPs) from adult rat serum and molecular cloning of a novel IGFBP-5 in rat and human, *J. Biol. Chem. 266*, 10646−10653.
21. Yamanaka, Y., Wilson, E. M., Rosenfeld, R. G., and Oh, Y. M. (1997) Inhibition of insulin receptor activation by insulin-like growth factor binding proteins, *J. Biol. Chem. 272*, 30729−30734.
22. Kostecka, Y., and Blahovec, J. (1999) Insulin-lke growth factor binding proteins and their functions, *Endocr. Regul. 33*, 90−94.
23. Yarden, Y., and Ullrich, A. (1988) Growth factor receptor tyrosine kinases, *Annu. Rev. Biochem. 57*, 443−478.
24. Groppe, J., Greenwald, J., Wiater, E., Rodriguez-Leon, J., Economides, A., Kwiatkowski, W., Affolter, M., Vale, W., Belmonte, J., and Choe, S. (2002) Structural basis of BMP signaling inhibition by the cystine knot protein Noggin, *Nature 420*, 636−642.
25. Keil, B. (1992) *Specificity of Proteolysis*, p 335, Springer-Verlag, Berlin, Heidelberg, and New York.

BI036160F